

**Asymmetric Catalysis**

# Regiodivergent and Enantioselective Synthesis of Cyclic Sulfones via Ligand-Controlled Nickel-Catalyzed Hydroalkylation

 Chao Fan<sup>†</sup>, Uttam Dhawa<sup>†</sup>, Deyun Qian, Davor Sakic, Jennifer Morel, and Xile Hu\*

**Abstract:** Cyclic sulfones have demonstrated important applications in drug discovery. However, the catalytic and enantioselective synthesis of chiral cyclic sulfones remains challenging. Herein, we develop nickel-catalyzed regiodivergent and enantioselective hydroalkylation of sulfolenes to streamline the synthesis of chiral alkyl cyclic sulfones. The method has broad scope and high functional group tolerance. The regioselectivity can be controlled by ligands only. A neutral PYROX ligand favors C3-alkylation whereas an anionic BOX ligand favors C2-alkylation. This control is kinetic in origin as the C2-bound Ni intermediates are always thermodynamically more stable. Reactivity study of a wide range of relevant Ni intermediates reveal a Ni<sup>I</sup>/Ni<sup>III</sup> catalytic cycle with a Ni<sup>II</sup>-H species as the resting state. The regio- and enantio-determining step is the insertion of this Ni<sup>II</sup>-H species into 2-sulfolene. This work provides an efficient catalytic method for the synthesis of an important class of organic compounds and enhances the mechanistic understanding of Ni-catalyzed stereoselective hydroalkylation.

## Introduction

A large variety of small-molecules in clinical trials comprise of at least one ring system, due to its high potential to enhance physicochemical properties of drug candidates.<sup>[1]</sup> Sulfur-containing compounds, particularly with S(VI) centers, have found applications in medicinal, agrochemical and material science.<sup>[2]</sup> Structurally, sulfones are regarded as

bioisosteres of ketones and carboxylic acids, and possess unique physical properties while providing enhanced binding affinity with the targeted proteins by non-covalent hydrogen bond interactions. Enantioenriched cyclic sulfones and their derivatives have demonstrated important biological activities (Figure 1a).<sup>[3]</sup> Despite their significant importance, methods for the efficient synthesis of cyclic sulfone derivatives are currently limited. This situation reflects the difficulty in the functionalization of cyclic sulfones compared to *N*, and *O*-based heterocycles.<sup>[4]</sup>

Asymmetric hydrogenation, cyclization, or cycloaddition methods have been reported for the synthesis of chiral cyclic sulfones. These methods frequently require lengthy synthesis of precursors (Figure 1b).<sup>[5]</sup> Direct functionalization of preformed and readily available cyclic sulfone represents a more versatile approach, but there are only few precedents.<sup>[6]</sup> A notable example is the rhodium-catalyzed enantioselective hydroarylation of 3-sulfolene reported by the Hayashi group (Figure 1b).<sup>[6d]</sup> As Ni-catalyzed enantioselective hydroalkylation of alkenes emerges as a versatile method in C(sp<sup>3</sup>)-C(sp<sup>3</sup>) bond formation,<sup>[7]</sup> we considered such a method for the synthesis of chiral alkyl-substituted sulfones from sulfolenes.

Although there is significant progress in Ni-catalyzed enantioselective hydroalkylation and related hydrofunctionalization reactions,<sup>[8]</sup> achieving simultaneously regio- and enantioselectivity is challenging. Typically, the regioselectivity is dictated by the nature of directing groups, or by the stability of the metallocycle intermediate.<sup>[9]</sup> The selectivity cannot be easily altered within one given system. The Lu group reported a pioneering study where temperature was used as a control to achieve regiodivergent alkene hydroalkylation<sup>[10]</sup> (Figure 1c). At 100 °C, a five-membered nickelocycle is more stable than its six-membered counterpart, so alkylation is selective at the  $\alpha$ -site to the amide directing group. At 10 °C, the six-membered nickelocycle is more stable, giving  $\beta$ -alkylation. The Rong group then reported enantioselective and regiodivergent hydroalkylation of pyrrolines by switching the catalytic metal.<sup>[11]</sup> The Ni-H catalysis yielded C2-alkylation, whereas the Co-H catalysis yielded C3-alkylation. A similar strategy was used by the Shu group to obtain regiodivergent and enantioselective hydroamination using either a Ni-H or a Cu-H catalyst.<sup>[8c]</sup> Despite this progress, regiodivergent hydroalkylation of electron-deficient conjugated alkenes remained elusive, because it would be difficult to overcome the innate regioselectivity due to the electronic properties of the substrates. Moreover, prior to this work, ligand-controlled simultaneously regiodivergent and enantioselective hydro-

[\*] Dr. C. Fan,<sup>†</sup> Dr. U. Dhawa,<sup>†</sup> Prof. Dr. D. Qian, J. Morel, Prof. Dr. X. Hu  
 Laboratory of Inorganic Synthesis and Catalysis, Institute of Chemical Sciences and Engineering, École Polytechnique Fédérale de Lausanne, ISIC-LSCI, BCH 3305, 1015 Lausanne, Switzerland  
 E-mail: xile.hu@epfl.ch  
 Homepage: lsci.epfl.ch

Prof. Dr. D. Sakic  
 University of Zagreb, Faculty of Pharmacy and Biochemistry, Ante Kovačića 1, 10000 Zagreb, Croatia

[†] These authors contributed equally to this work.

© 2024 The Authors. Angewandte Chemie International Edition published by Wiley-VCH GmbH. This is an open access article under the terms of the Creative Commons Attribution License, which permits use, distribution and reproduction in any medium, provided the original work is properly cited.

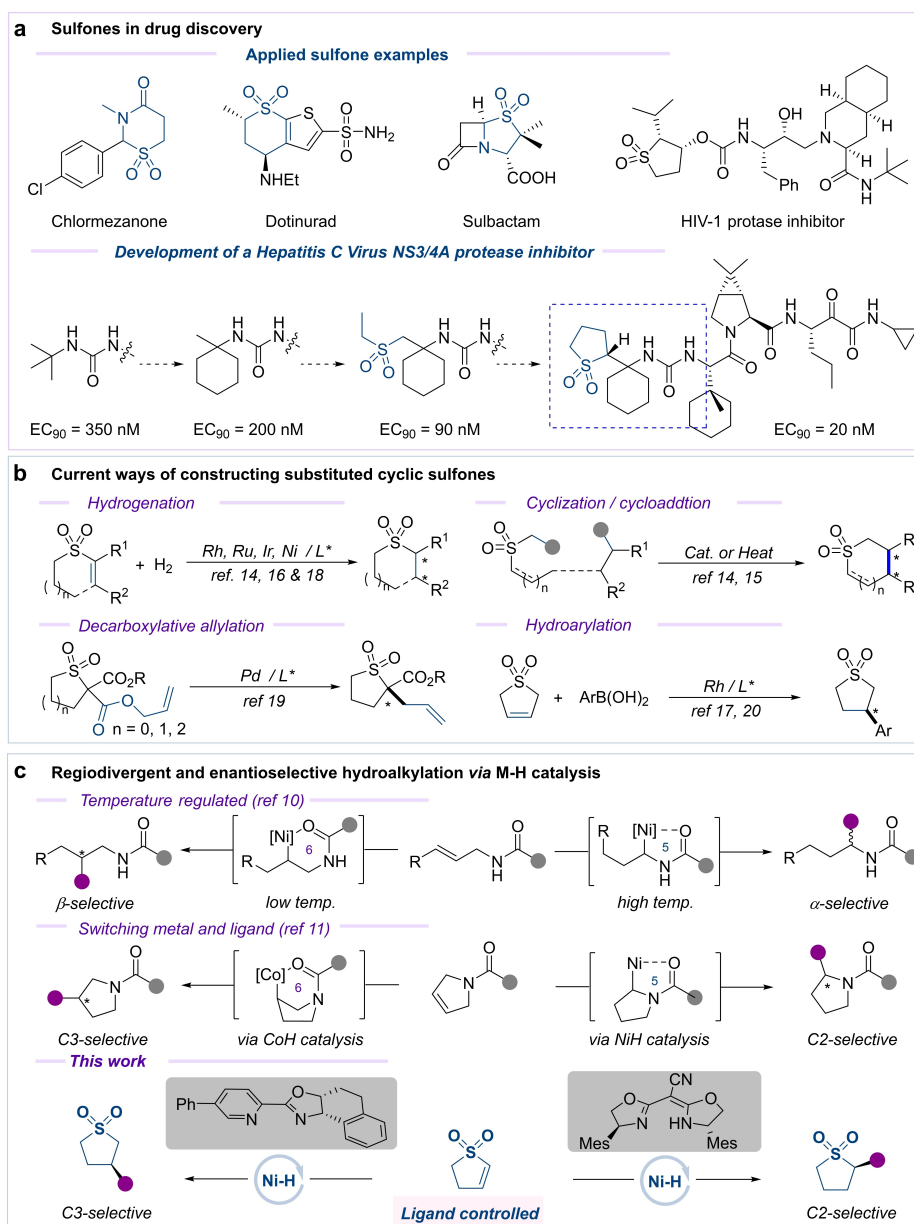


**Figure 1.** Synthesis of chiral cyclic sulfones via Ni–H catalyzed hydroalkylation. a. Selected examples of important cyclic sulfone in medicinal research. b. Previous examples on constructing chiral cyclic sulfones. c. Regiodivergent and enantioselective hydroalkylation and this work.

alkylation using identical substrates had not been reported, although racemic methods were known for amide-based substrates.<sup>[9c,d,12]</sup> Here we describe a method for Ni-catalyzed regiodivergent and enantioselective hydroalkylation of sulfones. By judicious choice of ligands, we can achieve either C2- or C3-alkylation in high regioselectivity and enantioselectivity in the same catalytic system. The method provides a rapid access to a large number of chiral cyclic sulfones from readily available reagents and with high functional group tolerance. Mechanistic study indicates a Ni<sup>I</sup>/Ni<sup>III</sup> catalytic cycle where the reactivity of the key intermediates has been determined.

## Results and Discussion

We started our investigation by optimizing reaction conditions for regio- and enantioselective hydroalkylation of the 2-sulfolene (**1a**) with a primary alkyl iodide (**2a**) (Table 1a and Supporting Information Table. S1–S5). We found that the reactions of **1a** had better regioselectivity than those of **1b**, its regioisomer (see below). Compound **1a** can be easily synthesized in gram-scale by base-promoted isomerization of **1b**. Among a representative set of ligands, PYROX ligands stood out for C3-selective alkylation. The ligand **L1** provided the desired product **3a** with 70% yield and 88:12 *er* under the following reaction conditions: Ni(NO<sub>3</sub>)<sub>2</sub>·6H<sub>2</sub>O (10 mol %), ligand (15 mol %), K<sub>3</sub>PO<sub>4</sub>/PhMe-

**Table 1:** Optimization of reaction conditions. <sup>a</sup> See the Supporting Information for experimental details; all reactions were carried out on 0.1 mmol scale with respect to **1a**; GC yields (calibrated using *n*-decane as an internal standard) and regioisomeric ratio (*rr*) were reported. <sup>b</sup> The enantiomeric ratios (*er*) were determined using chiral HPLC analysis of the product after column chromatography. <sup>c</sup> Isolated yield is shown in the parenthesis. DMA = *N,N*-Dimethylacetamide.

**a) C3 - selectivity**

Entry <sup>a</sup>	Ligand	Deviation	Yield (%)	<i>er</i> <sup>b</sup> (3a)	<i>rr</i> <sup>a</sup> (3a/4a)
A1	L1	--	70	88:12	8:1
A2	L2	--	56	92:8	>10:1
A3	L3	--	83(73) <sup>c</sup>	95:5	>10:1
A4	L4	--	95	94:6	>10:1
A5	L5	--	25	88:12	>10:1
A6	L6	--	20	88:12	8:1
A7	L3	<b>1b</b>	42	80:20	10:1
A8	L3	@ 25 °C	70	88:12	10:1
A9	L3	@ -10 °C	30	97:3	>10:1
A10	L3	NiCl <sub>2</sub> -DME	52	95:5	>10:1
A11	L3	Me <sub>2</sub> (MeO)SiH	54	88:12	8:1
A12	L3	Ph <sub>2</sub> (MeO)SiH	45	86:14	6:1

**b) C2 - selectivity**

Entry <sup>a</sup>	Ligand	Deviation	Yield (%)	<i>er</i> <sup>b</sup> (4a)	<i>rr</i> <sup>a</sup> (4a/3a)
B1	L7	--	5	77:23	1:3
B2	L8	--	15	90:10	1.2:1
B3	L9	--	trace	--	--
B4	L10	--	81	89:11	1.2:1
B5	L11	--	88	94:6	8:1
B6	L12	--	95(78) <sup>c</sup>	98:2	single
B7	L12	<b>1b</b>	82	93:7	1.3:1
B8	L12	NiI <sub>2</sub> ·xH <sub>2</sub> O	45	95:5	10:1
B9	L12	(EtO) <sub>3</sub> SiH	89	97:3	10:1
B10	L12	HBpin	95	96:4	10:1

(OMe)SiH (2.5 equiv.) and DMA (0.2 M) under 0 °C for 48 hours. Modification of the oxazole backbone from five-membered ring to six-membered ring (**L2**) resulted in lower yield but higher enantioselectivity (entry A1 vs entry A2). Gratifyingly, introduction of a phenyl group on the 4-position of the pyridine ring (**L3**) led to high enantioselectivity (95:5 *er*) and excellent yield (83 %) (entry A3).

Installation of a bromo group on the oxazoline motif (**L4**) increased further the yield (95 %) but decreased slightly the enantioselectivity (94:6 *er*). A PYROX ligand with a larger bite angle (**L5**) or a chiral diamine (**L6**) gave low yields (entries A5–A6). When **1b** was used as the substrate instead of **1a**, the yield (42 %) and the *er* (80:20) were much lower (entry A7). For further experiments, we

selected **L3** as the optimized ligand for C3-selective alkylation of 2-sulfolene. Additional experiments showed that another nickel salt, lower or higher temperature, or other silanes were less effective (entries A8–A12). Note that in all these cases, the C3-alkylation was dominant.

Next, we turned to optimize the reaction conditions for C2-selective hydroalkylation of cyclic sulfolenes (Table 1b and Supporting Information Table. S6–S9). We found that bi-oxazoline and bis-oxazoline ligands (**L7–L12**) were able to promote C2-alkylation. The reaction protocol was NiBr<sub>2</sub>·diglyme (10 mol %), ligand (15 mol %), Na<sub>2</sub>CO<sub>3</sub>/(EtO)<sub>2</sub>MeSiH (2.5 equiv.) and DMA (0.1 M) under room temperature for 24 hours. With neutral ligands **L7–L8**, the yields were very low (Table 1B, entries B1–B2). Although

the anionic BOX ligand **L9** gave no yield (entry B3), cyano-substituted BOX ligand<sup>[13]</sup> **L10** gave a good yield of 81% and good *er* of 89:11 (entry B4). But in this case the C2:C3 regioselectivity was only 1.2:1. Fortunately the regioselectivity could be improved by varying the substituent of the BOX ligands. A change from benzyl to phenyl (**L11**) increased the regioselectivity to 8:1 (entry B5). Further change from the phenyl group to a bulkier mesityl group (**L12**) then resulted in complete C2-selectivity, as well as a high yield (95%) and high enantioselectivity (98:2 *er*) (entry B6). Again, the use of the sulfolene isomer **1b** instead of **1a** led to poor regioselectivity (1.3:1) (entry B7). The use of NiI<sub>2</sub>·xH<sub>2</sub>O as Ni salt lowered the yield (entry B8), but the use of other reactive hydride donors such as (EtO)<sub>3</sub>SiH and HBpin gave similar results as (EtO)<sub>2</sub>MeSiH (entries B9–10).

With optimized conditions in hand (entry A3, Table 1a), we examined the substrate scope of the C3-selective hydroalkylation of 2-sulfolene (Figure 2). A broad range of alkyl iodides were suitable coupling partners, and functional groups such as chloro-, bromo-, iodo- and boryl group were well compatible, affording the C3-alkylated sulfones **3b–3e** in good yields and with good to high enantioselectivities. In the case of **2d**, a notable amount of arylation product (**3d'**) was observed as by-product (~15%, see Supporting Information), and a drop in the enantioselectivity was detected

for the C3-alkylated sulfone **3d**, possibly due to a competing catalytic cycle. We observed an influence of halogen bonding interaction when bromo containing chiral ligand **L4** was used instead of **L3** for certain substrates. For instance, for alkyl iodide **2c**, the enantioselectivity increased from 91:9 *er* to 97:3 *er* with **L4** as the ligand. Electrophilic functional groups such as nitrile and triflate were also tolerated, delivering the corresponding enantioenriched C3-alkylated products **3f–3g**. Substrates containing a free phenol (**2h**) and an alkyl alcohol (**2i**) reacted to give C3-alkylated products (**3h** and **3i**) in high enantioselectivity but the yields were reduced to about 50%. A substrate containing an easily reducible ketone (**2j**) underwent alkylation with a high yield and enantioselectivity without suffering from possible ketone reduction by the nickel-hydride intermediate. The reaction of a bulky silyl protected alcohol **2k** had lower enantioselectivity (83:17 *er*). A Boc-protected amine **2l** was alkylated in 85% yield with 93:7 *er*. Importantly, heterocycles including phthalimide (**2m**), furan (**2n**) and thiophene (**2o**) were compatible under this reaction protocol, providing enantioenriched **3m–3o**. The 3-alkylation protocol was successfully applied to a substrate derived from indomethacin, a nonsteroidal anti-inflammatory drug. The desired C3-alkylated sulfone was obtained in 65% yield with 90:10 *er*. The absolute configuration of

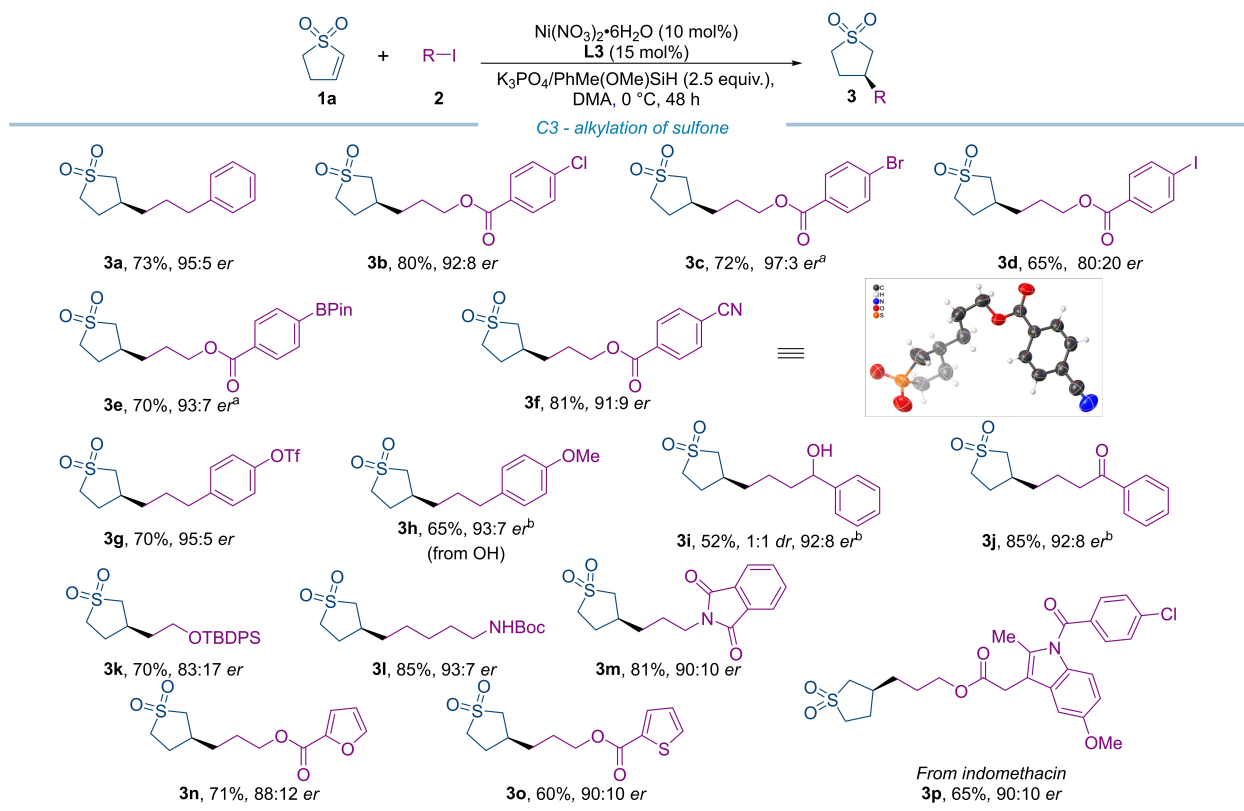


**Figure 2.** Reaction scope of nickel-catalysed enantio- and regioselective hydroalkylation for C3 selectivity. See the Supporting Information for experimental details (General procedure 1, GP1); all reactions were carried out on 0.1 mmol scale with respect to **1a**. Isolated yields are reported. The other regioisomer was unable to be isolated or detected. The enantiomeric ratios (*er*) were determined using chiral HPLC analysis of the product after column chromatography. <sup>a</sup> **L4** was used instead. <sup>b</sup> Enantiomeric ratio was determined after proper transformation. BPin = Boron pinacolate.

product **3f** was determined by X-ray crystallographic analysis. We assign a same absolute stereochemistry of the other C3-alkylated products based on this result.

We then tested the scope of C2-alkylation using the optimized protocol (entry B6, Table 1b). A wide range of alkyl iodides could be used, delivering enantioenriched, C2-alkylated sulfones **4** with high yields and enantioselectivities (Figure 3). A range of functional groups, including alkoxy- (**2b**), chloro- (**2c**), bromo- (**2d**), iodo (**2e**), triflate (**2f**) and boryl group (**2g**) were tolerated. Reaction of a substrate containing a phenol group (**2h**) again had a modest yield of 55 %, but the enantioselective was 99:1. Functional group such as ketone (**2i**), TBDPS protected alcohol (**2j**) and Cbz protected amine (**2k**) were all compatible. Likewise, alkyl iodides containing heterocycles like furan **2l**, thiophene **2m** and phthalimide **2n** were suitable coupling partners, affording the C2-alkylated sulfones in high enantioselectivity. The C2-selective reaction protocol was also used for the enantioselective synthesis of **4o** (50 % yield, 99:1 *er*). Note that the racemate of **4o** was found to be an antagonist for a neuropeptide receptor, but the bioactivity of each of its

enantiomers has not been yet studied. The synthesis of enantiomerically enriched **4o** opens the door for such a study.<sup>[14]</sup> Several complex alkyl iodide substrates derived from natural products and drugs were also successfully applied (**4p–4s**) and high enantioselectivity was obtained. The absolute configuration of product **4n** was determined by X-ray crystallographic analysis. We assign a same absolute stereochemistry of the other C2-alkylated products based on this result.

Radical clock experiments were performed under standard reaction conditions for both C2- and C3- selective alkylations. When 6-iodo-hex-1-ene (**5**) was used as a substrate, the cyclized products originated from intramolecular cyclization of the linear alkyl radical (hex-1-ene-6-yl) were obtained in both cases (Figure 4a and Supporting Information Figure S2). Addition of a radical scavenger 2,2,6,6-tetramethylpiperidine 1-oxyl (TEMPO) to the reaction medium inhibited the reaction, and an alkyl-TEMPO adduct was detected (Figure S4). These results indicate the involvement of an alkyl radical from an alkyl halide coupling partner in the catalysis. Deuterium labeling experiments

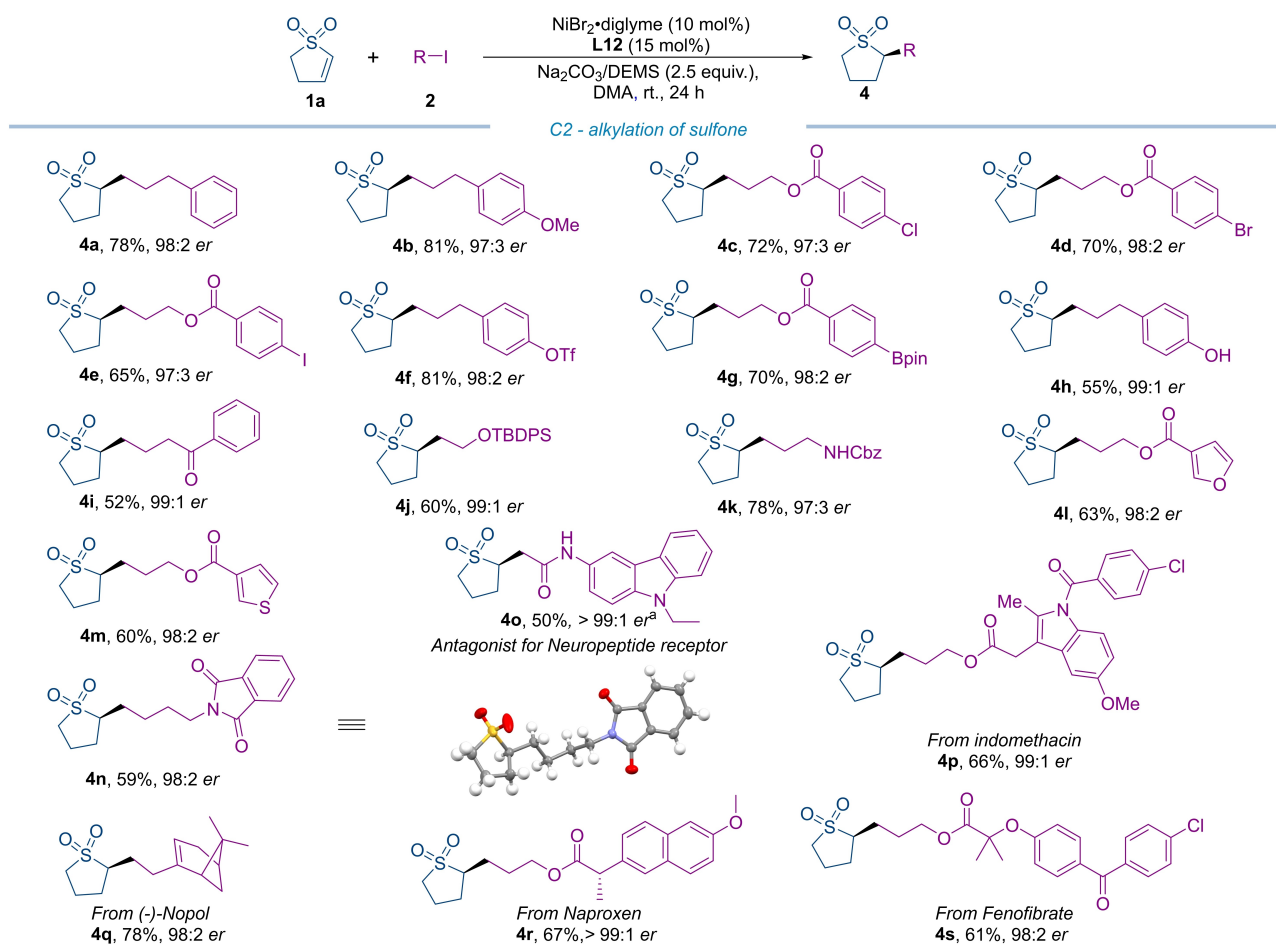


**Figure 3.** Reaction scope of nickel-catalysed enantio- and regioselective hydroalkylation for C2 selectivity. See the Supporting Information for experimental details (General procedure 2, GP2); all reactions were carried out on 0.1 mmol scale with respect to **1a**. Isolated yields are reported. **4** was obtained as the single isomer. The enantiomeric ratios (*er*) were determined using chiral HPLC analysis of the product after column chromatography. <sup>a</sup>Alkyl bromide was used instead, KI (1 equiv.) was added as an additive. BPin = Boron pinacolate.

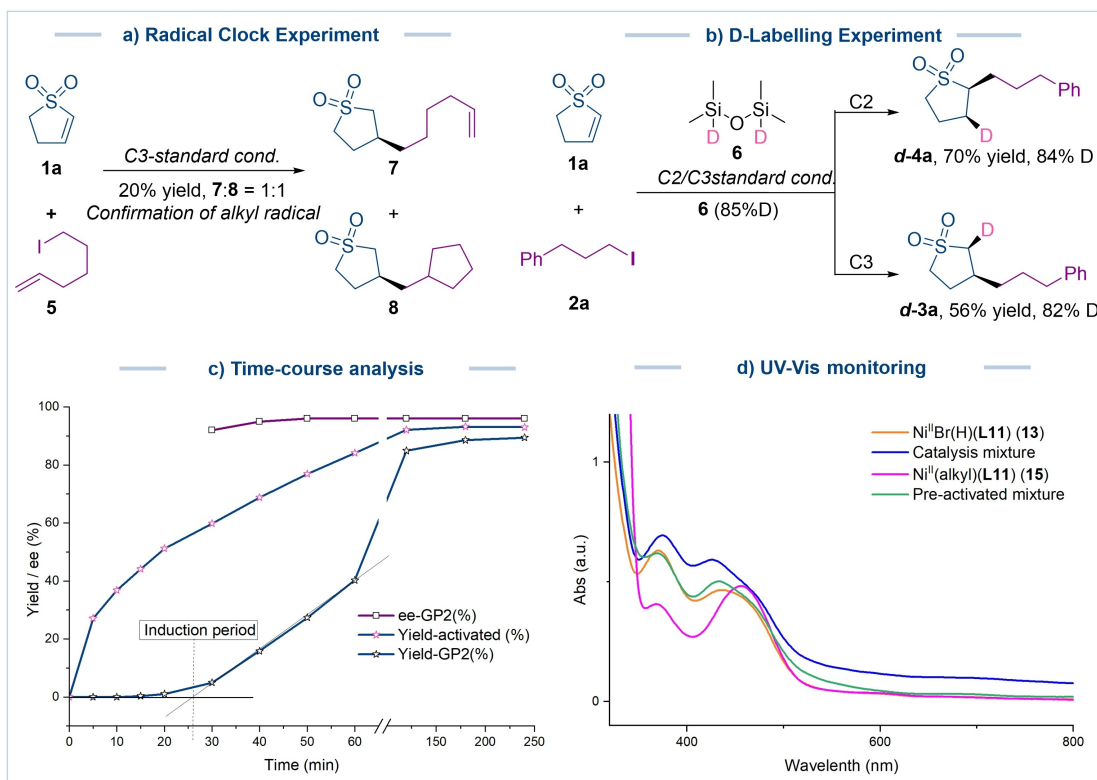


**Figure 4.** Mechanism study. a. Radical clock experiments under the standard reaction conditions. b. Deuterium labelling experiments under the standard reaction conditions. c. Time-course analysis for the standard reaction (GP2) and the pre-activated reaction. d. UV/Vis spectra of reaction mixture and relevant Ni complexes.

were performed using D-silane **6** (85 % D) as the source of hydride donor under otherwise identical reaction conditions. An almost quantitative deuterium incorporation was observed exclusively at the 3-position for C2-selective alkylation, and at the 2-position for C3-selective alkylation (Figure 4b). When a racemic **L12** was also used instead of its chiral version, the same result, that is, the D atom is always *cis* to the alkyl group, was obtained. These results indicate *syn*-addition of nickel-hydride to the alkenyl group. No deuterium scrambling was observed, suggesting that there is no homolytic cleavage and recombination of the Ni-alkyl bond. Moreover, the nickel-hydride addition into the C=C double bond is enantio-determining.

We conducted time-course and UV/Vis analyses. Under the standard condition, a 25-min induction period was observed (Figure 4c). We pre-mixed all the reaction components except the alkyl halide for 20 min. The reaction displayed no induction period after addition of the alkyl halide to the medium, and H<sub>2</sub> was detected in the headspace. When we used Ni(COD)<sub>2</sub> as the Ni source, an induction period of more than 90 minutes was observed (Figure S9), along with a significantly lower yield of 37% (vs. 88% in normal conditions). A previous DFT study suggests that a Ni<sup>0</sup> complex formed by reduction of a Ni<sup>II</sup> complex with a silane acts as the initial catalytic species.<sup>[15]</sup> Our data indicates that in our system the formation of a Ni<sup>0</sup> complex is not sufficient to initiate the catalysis.

A series of potential Ni<sup>0</sup>, Ni<sup>I</sup>, and Ni<sup>II</sup> intermediates were prepared (Supporting Information 5.5). Upon comparing their NMR spectra with that of the reaction mixture, we deduced that the latter belongs to a paramagnetic Ni<sup>II</sup> species. Further identification of this species by NMR was hindered by the broadness of the peaks (Figure S6). Subsequently, we used UV/Vis spectroscopy to investigate the species present in the reaction mixture. (Figure 4d) By comparing the spectrum of reaction mixture under the “normal” conditions after the induction period (blue) and that of the mixture generated by mixing all reagents except the alkyl iodide (the pre-activation mixture, green), we found that the resting state of Ni catalyst in the “normal” reaction is the same species that was generated during the pre-activation. Comparison of these spectra with those of independently prepared Ni<sup>II</sup> hydride (orange) and Ni<sup>II</sup> alkyl species (purple) indicates that the resting states likely consist of both Ni<sup>II</sup> hydride and Ni<sup>II</sup> alkyl species. When the pre-activated mixture was quenched by HCl solution, H<sub>2</sub> and sulfolane were formed in a ratio of 5:1, suggesting that in the resting state the ratio of Ni<sup>II</sup> hydride to Ni<sup>II</sup> alkyl species is 5 to 1. Further support for Ni<sup>II</sup> resting species came from the lack of EPR signal of Ni<sup>I</sup> species for the reaction mixture (Figure S8).

Both Ni<sup>0</sup>/Ni<sup>II</sup> and Ni<sup>I</sup>/Ni<sup>III</sup> catalytic cycles have been proposed for nickel hydride catalyzed hydroalkylation.<sup>[7]</sup> To probe these possibilities, we conducted a series of stepwise

reactions with pre-formed Ni<sup>I</sup> and Ni<sup>II</sup> halide, hydride, and alkyl species (**10–16**, Figure 5 and Supporting Information). In general, phosphine ligands or diamine ligands are needed to obtain a stable nickel hydride complex.<sup>[16]</sup> Bidentate ligands bearing oxazoline or pyridine which are the common ligands used in hydroalkylation<sup>[7]</sup> had not been reported to support nickel hydride species. Probably because the anionic

bisoxazoline ligand we use here has a large conjugate backbone that is similar to that of diimine ligands, we could for the first time obtain nickel hydride complexes in the solution for mechanistic study.

To assess the trapping of an alkyl radical intermediate by a nickel alkyl species before alkyl-alkyl reductive elimination, we generated an alkyl radical by photolysis of tert-

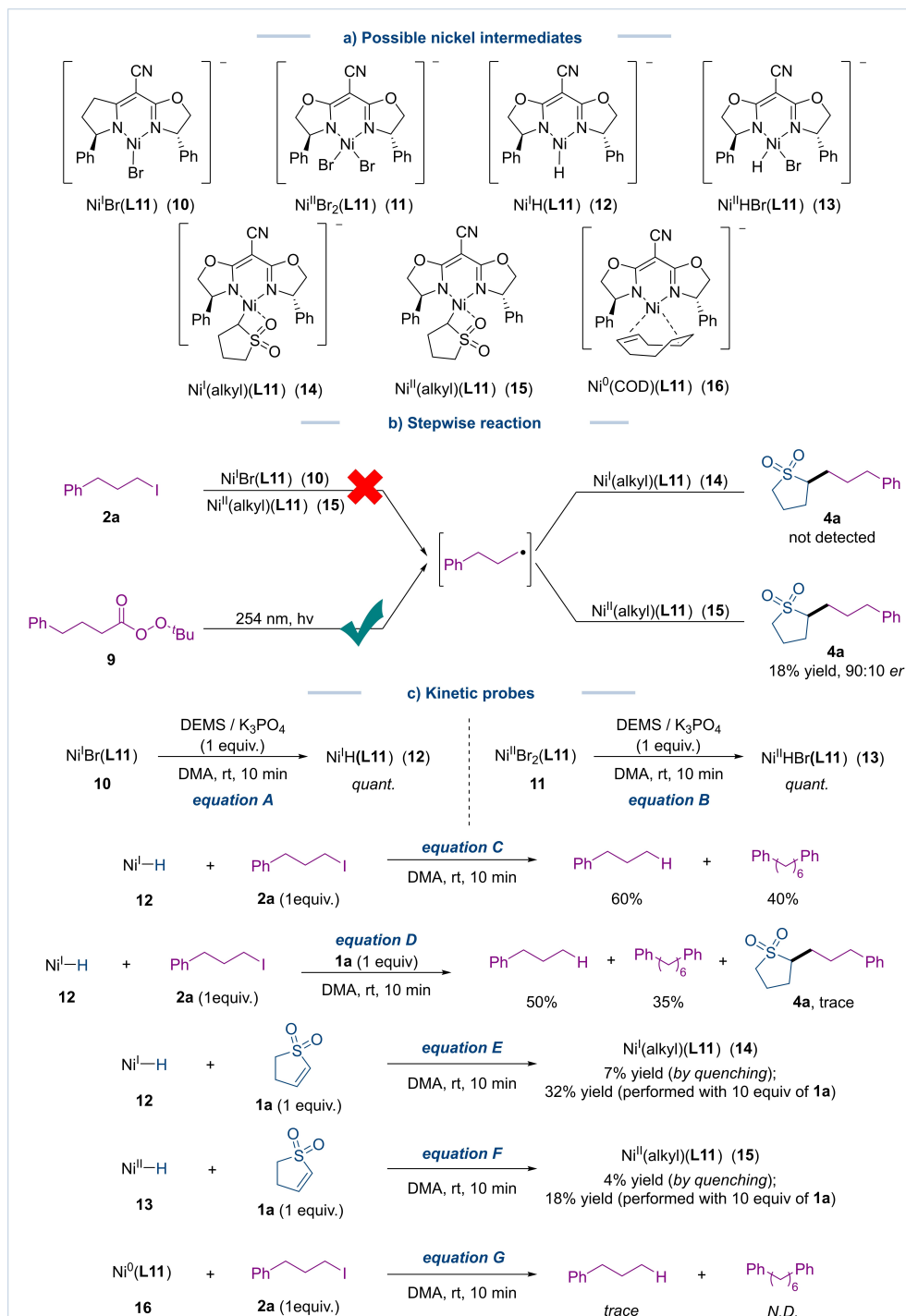


**Figure 5.** Reactivity study. a. Possible nickel intermediates. b. Radical activation and radical capture reactions. c. Kinetic probes to compare reaction rates between major steps in possible catalytic cycle.

Butyl  $\gamma$ -phenylperoxybutyrate **9** (Figure 5b).<sup>[17]</sup> In the presence of the Ni<sup>II</sup> alkyl species **15**, the formation of the hydroalkylation product **4a**, albeit in a low yield, indicates that Ni<sup>II</sup> alkyl species was able to capture an alkyl radical to form a Ni<sup>III</sup> bis(alkyl) species before reductive elimination. In contrast, in the presence of the Ni<sup>I</sup> alkyl species **14**, no hydroalkylation product was formed. These results support a Ni<sup>I</sup>/Ni<sup>III</sup>, rather than a Ni<sup>0</sup>/Ni<sup>II</sup> catalytic cycle.

The Ni<sup>I</sup> halide species (**10**), which is often suggested as an activator of an alkyl halide,<sup>[18]</sup> did not react with the alkyl iodide **2a**. Likewise, the Ni<sup>II</sup>-alkyl species (**15**) failed to react with **2a**. Thus, these species could not be responsible for the activation of alkyl halide. On the other hand, Ni<sup>0</sup>, Ni<sup>I</sup> and Ni<sup>II</sup> hydride, as well as Ni<sup>I</sup> alkyl could all activate **2a**, although the reaction rates were very different (Figure 5c, equations C, G and Figure S11, Supporting Information). It was found that within 10 min at room temperature, the formation of Ni<sup>I</sup> or Ni<sup>II</sup> hydride (**12** or **13**) by reaction of their corresponding halide with the silane, as well as the activation of alkyl halide **2a** by the Ni<sup>I</sup> hydride (**12**) were already at full conversion (Figure 5c, equations A–C). In the presence of the alkene substrate **1a**, the reaction of **12** with **2a** occurred in a similar speed, but only a trace amount of hydroalkylation product **4a** was found (Figure 5c, equation D). This result suggests that Ni<sup>I</sup> hydride reacts much faster with an alkyl halide than with an alkene. Indeed, reaction of **12** with the alkene **1a** had only 7% yield after 10 min (Figure 5c, equation E). On the other hand, reaction of Ni<sup>II</sup> hydride (**13**), or Ni<sup>0</sup> (**16**) with **2a** was quite slow and had little conversion after 10 min (Figure 4c, equations G, and Figure S11, Supporting Information). The insertion of Ni<sup>II</sup> hydride **13** into alkene **1a** to give Ni<sup>II</sup> alkyl is also slow, with a 4% yield after 10 min (Figure 5c, equations F). The above results indicate that Ni<sup>I</sup> hydride (**12**) is the species that activate alkyl halide and the resulting Ni<sup>II</sup> hydride (**13**) is the resting state. The insertion of **13** into the alkene is then the rate-determining step.

Based on the above results and previous mechanistic studies of related reactions,<sup>[7,15]</sup> we propose a Ni<sup>I</sup>/Ni<sup>III</sup> catalytic cycle for the C2-selective alkylation as shown in Figure 6. The mixing of a Ni<sup>II</sup> salt with the ligand gives a Ni<sup>II</sup>-halide species (**A**), which would immediately react with a silane in the presence of a base to give a Ni<sup>II</sup>-H species (**B**), which is the main resting species of the reaction. Insertion of **B** into the alkene **1a** gives a Ni<sup>II</sup>-alkyl species (**F**). Both the enantioselectivity and regioselectivity are set at this migratory insertion step. Meanwhile, in this reducing reaction environment, some Ni<sup>II</sup>-H species would react further with the silane and decompose to a Ni<sup>0</sup> species (**C**). The latter can activate the alkyl halide to generate an alkyl radical, thereby initiating the catalysis. This process explains the induction period observed in the normal reaction, and the lack of an induction period when the reagents except alkyl halide were pre-mixed. Once generated, the alkyl radical can be captured by the Ni<sup>II</sup>-alkyl species (**F**) to form a Ni<sup>III</sup> bis(alkyl) intermediate (**G**). C–C reductive elimination from **G** affords the hydroalkylation product and a Ni<sup>I</sup> halide (**D**), which reacts quickly with the silane in the presence of base to form a Ni<sup>I</sup> hydride **E**. Species **E** now

reacts quickly with the alkyl halide to give the alkyl radical and the Ni<sup>II</sup> hydride species **B**, thereby closing the catalytic cycle. Alternatively, the Ni<sup>0</sup> species (**C**) could react with the Ni<sup>II</sup> species (**A** or **B**) to form Ni<sup>I</sup> halide (**D**) or Ni<sup>I</sup> hydride (**E**) species,<sup>[7]</sup> thereby entering the catalytic cycle. The C3-alkylation should follow a similar mechanism except that the insertion of Ni<sup>II</sup> hydride into 2-sulfolene gives a C3-bound Ni alkyl intermediate.

Although the C2- versus C3-selectivity reported here can be easily attributed to the influence of the ligands, it is not clear whether this influence is thermodynamic or kinetic in origin. To probe this question, we conducted density functional theory (DFT) calculations of the relevant C2- and C3-bound Ni<sup>II</sup> alkyl intermediates (Figure 5b). We found that regardless of the ligands, the C2-bound Ni<sup>II</sup> alkyl intermediates are about 10 kcal/mol more stable than the C3-bound intermediates. The C3-selectivity observed using the PY-ROX ligand, thus, is a kinetic product. A complete DFT study, including the calculations of activation barriers for the reaction profile, is subject to future work.

## Conclusion

In summary, a regiodivergent and enantioselective method has been developed for Ni-catalyzed hydroalkylation of sulfolenes. This method provides a rapid access to a large number of enantiomerically enriched cyclic sulfones that are otherwise difficult to make. The method has a high functional group tolerance. The regioselectivity can be switched from C3-selective to C2-selective using two different sets of ligands. This control of regioselectivity is kinetic in origin, as the C2-bound Ni alkyl intermediate formed by insertion of a Ni hydride into 2-sulfolene is more stable than its C3-counterpart regardless of the ligands. With ligand L11, the corresponding Ni<sup>I</sup> and Ni<sup>II</sup> hydride and alkyl species could be cleanly formed and their reactivity could be studied. The corresponding data indicate a Ni<sup>I</sup>/Ni<sup>III</sup> catalytic cycle where the nature of the key intermediates has been elucidated. In addition to synthetic applications, we expect the study to enhance the mechanistic understanding of Ni-catalyzed hydroalkylation.

## Supporting Information

Experimental procedures, and compound characterization data that support the findings of this study are available in the online version of this paper in the accompanying Supporting Information. Crystallographic data for **3f** and **4n** have been deposited at the Cambridge Crystallographic Data Centre, under deposition numbers CCDC 2291816 (**3f**), CCDC 2241636 (**4n**). Copies of the data can be obtained free of charge via [www.ccdc.cam.ac.uk](http://www.ccdc.cam.ac.uk). Further data are available online in Zenodo: doi: 10.5281/zenodo.11065419.



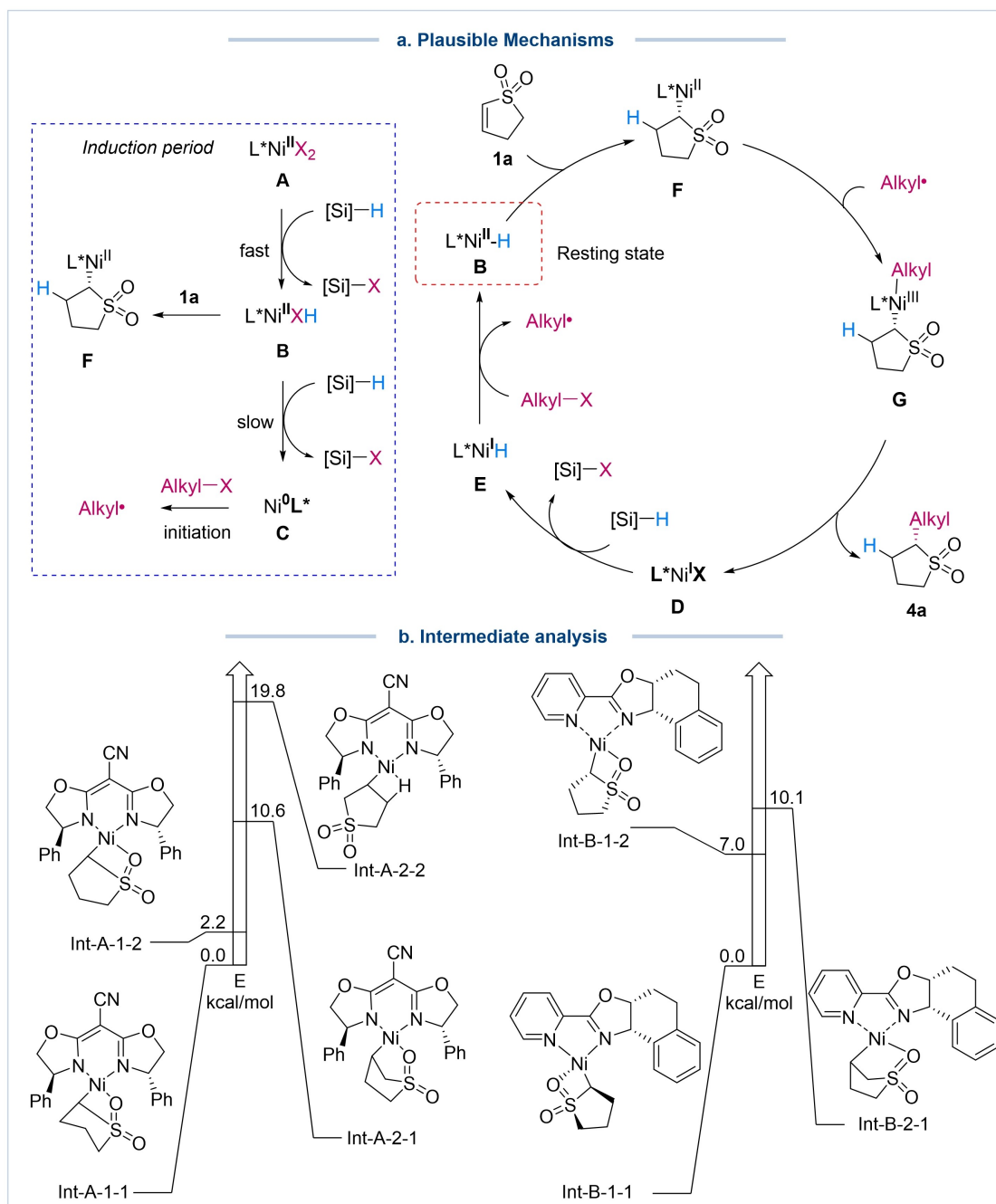


Figure 6. Catalytic cycle and DFT analysis.

### Acknowledgements

This work is supported by the Swiss National Science Foundation (no. 200020\_212062). We thank Dr. Rosario Scopelliti (EPFL) and Dr. Farzaneh Fadaei Tirani (EPFL) for the determination of the X-ray crystal structure of compounds **3f** and **4n**. Open Access funding provided by École Polytechnique Fédérale de Lausanne.

### Conflict of Interest

The authors declare no conflict of interest.

### Data Availability Statement

The data that support the findings of this study are openly available in Zenodo at <https://doi.org/10.5281/zenodo.11065419>, reference number [11102723].

**Keywords:** Asymmetric catalysis · regiodivergent · heterocycles · hydroalkylation · nickel

- [1] a) D. F. Veber, S. R. Johnson, H.-Y. Cheng, B. R. Smith, K. W. Ward, K. D. Kopple, *J. Med. Chem.* **2002**, *45*, 2615–2623; b) S. D. Roughley, A. M. Jordan, *J. Med. Chem.* **2011**, *54*, 3451–3479.
- [2] a) D. J. Ager, D. P. Pantaleone, S. A. Henderson, A. R. Katritzky, I. Prakash, D. E. Walters, *Angew. Chem. Int. Ed.* **1998**, *37*, 1802–1817; b) J. Dong, K. B. Sharpless, L. Kwisnek, J. S. Oakdale, V. V. Fokin, *Angew. Chem. Int. Ed.* **2014**, *53*, 9466–9470; c) J.-Y. Winum, A. Scozzafava, J.-L. Montero, C. T. Supuran, *Med. Res. Rev.* **2006**, *26*, 767–792.
- [3] a) M. Feng, B. Tang, H. S. Liang, X. Jiang, *Curr. Top. Med. Chem.* **2016**, *16*, 1200–1216; b) F. Zhao, J. Wang, X. Ding, S. Shu, H. Liu, *Chin. J. Org. Chem.* **2016**, *36*, 490–501; c) A. Regueiro-Ren, *Chapter One – Cyclic sulfoxides and sulfones in drug design. in Adv. Heterocycl. Chem.* (eds. N. A. Meanwell, M. L. Lolli) vol. 134, 1–30, Academic Press, **2021**; d) F. Velázquez, M. Sannigrahi, F. Bennett, R. G. Lovey, A. Arasappan, S. Bogen, L. Nair, S. Venkatraman, M. Blackman, S. Hendrata, Y. Huang, R. Huelgas, P. Pinto, K.-C. Cheng, X. Tong, A. T. McPhail, F. G. Njoroge, *J. Med. Chem.* **2010**, *53*, 3075–3085; e) L. Navarro, G. Rosell, S. Sánchez, N. Boixareu, K. Pors, R. Pouplana, J. M. Campanera, M. D. Pujol, *Bioorg. Med. Chem.* **2018**, *26*, 4113–4126.
- [4] a) T. Punniyamurthy, A. Kumar, *Transition-Metal-Catalyzed C–H Functionalization of Heterocycles*, Wiley-VCH, **2023**; b) J. A. Joule, K. Mills, *Heterocycl. Chem.*, 5th Edition (Wiley-Blackwell, 2010).
- [5] a) C. Zhu, Y. Cai, H. Jiang, *Org. Chem. Front.* **2021**, *8*, 5574–5589; b) Y. Huang, J. Li, H. Chen, Z. He, Q. Zeng, *Chem. Rec.* **2021**, *21*, 1216–1239; c) X. Liang, Y. Shen, *Asian J. Org. Chem.* **2022**, *11*, e202100598; d) T. Zhou, B. Peters, M. F. Maldonado, T. Govender, P. G. Andersson, *J. Am. Chem. Soc.* **2012**, *134*, 3201–3204.
- [6] a) F. de Azambuja, R. C. Carmona, T. H. D. Chorro, G. Heerdt, C. R. D. Correia, *Chem. Eur. J.* **2016**, *22*, 11205–11209; b) F. Hu, J. Jia, X. Li, Y. Xia, *Org. Lett.* **2021**, *23*, 896–901; c) E. Bowen, G. Laidlaw, B. C. Atkinson, T. A. McArdle-Ismaguilov, V. Franckevicius, *J. Org. Chem.* **2022**, *87*, 10256–10276; d) K. M.-H. Lim, T. Hayashi, *J. Am. Chem. Soc.* **2015**, *137*, 3201–3204.
- [7] For reviews, see: a) Z. Zhang, S. Bera, C. Fan, X. Hu, *J. Am. Chem. Soc.* **2022**, *144*, 7015–7029; b) Y. He, J. Chen, X. Jiang, X. S. Zhu, *Chin. J. Chem.* **2022**, *40*, 651–661. For selected examples, see: c) Z. Wang, H. Yin, G. C. Fu, *Nature* **2018**, *563*, 379–383; d) F. Zhou, Y. Zhang, X. Xu, S. Zhu, *Angew. Chem. Int. Ed.* **2019**, *58*, 1754–1758; e) S.-J. He, J.-W. Wang, Y. Li, Z.-Y. Xu, X.-X. Wang, X. Lu, Y. Fu, *J. Am. Chem. Soc.* **2020**, *142*, 214–221; f) S. Bera, R. Mao, X. Hu, *Nat. Chem.* **2021**, *13*, 270–277; g) S. Bera, C. Fan, X. Hu, *Nat. Catal.* **2022**, *5*, 1180–1187; h) Q. Huang, Y. Chen, X. Zhou, L. Dai, L. Y. Lu, *Angew. Chem. Int. Ed.* **2022**, *61*, e202210560; i) C. Chen, W. Guo, D. Qiao, S. Zhu, *Angew. Chem. Int. Ed.* **2023**, *62*, e2023083; j) C. Chen, W. Guo, D. Qiao, J. Zhou, Y. Wang, S. Zhu, *CCS Chem.* **2023**, doi: 10.31635/ccschem.023.202303440.
- [8] a) Y. Wang, Y. He, S. Zhu, *Acc. Chem. Res.* **2023**, *56*, 3475–3491; b) J. Rodrialvarez, F.-L. Haut, R. Martin, *JACS Au* **2023**, *3* 3270–3282; c) Z.-X. Wang, B.-J. Li, *Angew. Chem. Int. Ed.* **2022**, *61*, e202201099; d) M. Liu, H. Shi, X. Meng, R. He, J. Huang, J. Wang, J. Lv, C. Wang, *CCS Chem.* **2023**, doi: 10.31635/ccschem.023.202303288; e) S. Wang, L. Shi, X.-Y. Chen, W. Shu, *Angew. Chem. Int. Ed.* **2023**, *62*, e202303795; f) L. Xie, J. Liang, H. Bai, X. Liu, X. Meng, Y.-Q. Xu, Z.-Y. Gao, C. Wang, *ACS Catal.* **2023**, *13*, 10041–10047; g) W.-T. Zhao, H. Meng, J.-N. Lin, W. Shu, *Angew. Chem. Int. Ed.* **2023**, *62*, e202215779; h) J.-S. Yang, K. Lu, C.-X. Li, Z.-H. Zhao, F.-M. Zhang, X.-M. Zhang, Y.-Q. Tu, *J. Am. Chem. Soc.* **2023**, *145*, 22122–22134.
- [9] a) C. Najera, I. P. Beleskaya, M. Yus, *Chem. Soc. Rev.* **2019**, *48*, 4515–4618; b) X.-X. Wang, Y.-T. Xu, Z.-L. Zhang, X. Lu, X. Y. Fu, *Nat. Commun.* **2022**, *13*, 1890; c) L. Zhao, Y. Zhu, M. Liu, L. Xie, J. Liang, H. Shi, X. Meng, Z. Chen, J. Han, C. Wang, *Angew. Chem. Int. Ed.* **2022**, *61*, e202204716; d) P.-F. Yang, W. Shu, *Angew. Chem. Int. Ed.* **2022**, *61*, e202208018; e) Z. Li, B. Liu, C.-Y. Yao, G.-W. Gao, J. Y. Zhang, Y.-Z. Tong, J.-X. Zhou, H.-K. Sun, Q. Liu, X. Lu, Y. Fu, *J. Am. Chem. Soc.* doi: 10.1021/jacs.3c12881.
- [10] J.-W. Wang, D.-G. Liu, Z. Chang, Z. Li, Y. Fu, X. Lu, *Angew. Chem. Int. Ed.* **2022**, *61*, e202205537.
- [11] X. Wang, J. Xue, Z.-Q. Rong, *J. Am. Chem. Soc.* **2023**, *145*, 15456–15464.
- [12] D. Qian, X. Hu, *Angew. Chem. Int. Ed.* **2019**, *58*, 18519–18523.
- [13] Z. Li, H. Shi, X. Chen, L. Peng, Y. Li, G. Yin, *J. Am. Chem. Soc.* **2023**, *145*, 13603–13614.
- [14] M. Howard, S. Craig, K. Foote, P. Schofield, P. Robert, World Patent WO WO2001007409 February 1, **2001**.
- [15] W. Xu, G. Pei, Y. Liu, S. Song, J. Li, *J. Mol. Catal.* **2022**, *552*, 112238.
- [16] N. A. Eberhardt, H. Guan, *Chem. Rev.* **2016**, *116*, 8373–8426.
- [17] J. Breitenfeld, J. Ruiz, M. Wodrich, X. Hu, *J. Am. Chem. Soc.* **2013**, *135*, 12004–12012.
- [18] C. Wagner, G. Herrera, Q. Liu, C. Hu, T. Diao, *J. Am. Chem. Soc.* **2021**, *143*, 5295–5300.

Manuscript received: April 9, 2024

Accepted manuscript online: April 29, 2024

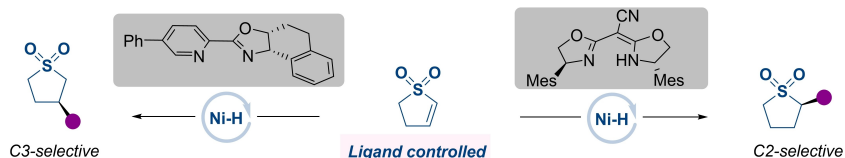
Version of record online: ■■■■■

## Research Articles

## Asymmetric Catalysis

C. Fan, U. Dhawa, D. Qian, D. Sakic,  
J. Morel, X. Hu\* [e202406767](#)

Regiodivergent and Enantioselective Synthesis of Cyclic Sulfones via Ligand-Controlled Nickel-Catalyzed Hydroalkylation



A ligand-controlled nickel catalyzed regiodivergent and enantioselective hydroalkylation of cyclic sulfone has been developed. A range of structurally diverse and enantioenriched C2 or C3 substi-

tuted cyclic sulfones are conveniently synthesized by this method. Detailed mechanistic studies indicated a Ni<sup>I</sup>/Ni<sup>III</sup> catalytic cycle.